Iranian Journal of Physics Research, Vol. 23, No. 3, 2023
DOI: 10.47176/ijpr.22.3.61487

Ni doped ZnO nanorod/glass prepared by chemical bath deposition

Hadeel A. Jameel Aljanaby and Hussein Abdullah Alshamarti

Department of Physics,College of Science, University of Kufa

E-mail: hadeel.rahman.1996@gmail.com

(Received 24 June 2022 ; in final form 7 June 2023)

Abstract

In this paper, Ni-doped ZnO nanorods (NRs) with concentrations of (0%, 1%, 2%, and 4%) were successfully grown on glass slides by Chemical bath deposition CBD at (85-90) °C. X-ray diffraction (XRD), Field Emission Scanning Electron Microscopy (FESEM), and UV- Vis spectrum were performed to characterize the prepared films. The results of the X-ray diffraction measurements of the samples showed that all the prepared films were of a crystalline structure of the hexagonal type with the dominance of growth in the (002) direction and a decrease in the intensity of the peak characteristic with increased Ni-doped. The FESEM images show the average diameters of ZnO NRs, Ni (1%) NRs, Ni (2%) NRs and Ni (4%) NRs, there is a clear increase in the rate of the average diameters by increasing the percentage of doping. The band gap of seed layers ZnO and undoped ZnO nanorods /glass was found to be 3.25 eV and 3.2 eV respectively. The values of the optical energy gap of Ni-doped ZnO are about (3.12, 3.09, 3) eV with an increase in the rate of doping. The results of the optical and structure measurements also included calculating parameters micro strain (ε), about the Ni doped ZnO (0%, 1%, 2%, and 4%) films for (100), (002), and (101).

Keywords: ZnO, seed; layer; CBD method; Ni-doped ZnO; nanorod

1. Introduction

ZnO nanostructures such as nanoparticles [1] , Nanorods (NRs) [2], nanowires [3],....etc.; were prepared in different shapes and dimensions through several studies that obtained different properties and applications [4]. The distinguishing feature of ZnO NRs nanomaterial is their large surface areas relative to their volume have many benefits for applications in photonics and electronics [5]. ZnO with a high exciton binding energy of about (60 meV), a wideband energy gap of (3.3 eV), high electrical conductivity, and great thermal stability [4] which has a major effect in some applications in optoelectronics such as LEDs [6], gas sensors [7], solar cells [8], transistors [9], and photo detector [6]. The preparation of zinc oxide Nanorods was chosen in this work because it has many specifications such as that it is non-toxic and low cost [10]. There are several research focused on efforts to control the properties of ZnO by adding various doping such as Cu [11], Al [12], Mn [13], Ag [14], Cd [15], Mg [16], and Ni [17] to control and adjust the test. ZnO doped with Ni has shown novel attention due to the strong correlation among the structural, optical, and magnetic properties [18], Because Ni+2 is believed to be the most promising and a candidate due to its close ionic radius of (0.069) nm against (0.074) nm for Zn+2 [19]. There are some results [18, 20] indicate that the presence of Ni alters the structural and optical properties of ZnO, while others indicate the size of nanoparticles [21]. It increases with the concentration of Ni. This apparent variance in the results could be described on the basis of the different synthesis methods used [17]. Synthesis of ZnO nanostructures and doped with Ni have been by various physical and chemical deposition techniques and several fabrication methods, such as molecular beam epitaxy [22], sol-gel method [23], pulsed laser deposition [1], a hydrothermal method [24] and chemical bath deposition [25], where CBD has been used to prepare ZnO nanostructures in our work due to its above-mentioned advantages**.** In recent periods, chemical bath deposition (CBD) has received a lot of attention and is commonly used to grow semiconductor nanostructures. The CBD method is a simple and inexpensive method and low-temperature wet chemistry has become a promising mechanism for the production of nanostructure on a large scale. According to the advantages of the chemical method mentioned above, it was used to prepare zinc oxide nanostructures and doped with different ratios of nickel, and study its properties structure, and optical for use in various applications.

2. Experimental procedures

ZnO NRs were grown on glass slips in the two stages by sol-gel and CBD methods [26]. The first step includes the

glass slips are cutting (2×2 cm) and their cleaning in three stages. They were cleaned by ultrasonically device with hydrochloric acid, acetone, and deionized water. The slides were placed in the glass beaker; the ultrasonic device was run for (3-5) minutes. Then they are dried at a temperature not exceeding (80) C° and placed in closed dishes to preserve them from external impurity. In the second step, a seed solution was prepared for coating the glass slides by dissolving an amount of zinc acetate Dehydrate (Zn ((CH3COO)2. 2H2O) with concentrations of (0.1) M in absolute ethanol. The solution is stirred for 3 hours at a temperature of (50-70) C°; stirring until a clear and homogeneous solution is obtained. In the third step, the cleaned glass slides were coated with the prepared seed solution with a rotation of 2000 rpm at room temperature, where evenly distributed on the surface of the glass slide. ZnO seed layers were dried at (150) C° for (10-12) min to remove the outer layer of organic waste. The above coating process was repeated more than once (5-8 times). then; the samples were annealed at (300-320) °C for 3 hours using an oven. Finally, the Ni-doped ZnO nanorods with concentrations of 0%, 1%, 2%, and 4% were prepared by the CBD method. The above substrate was placed perpendicularly in the beaker with an aqueous solution containing zinc nitrate hexahydrate Zn (NO3)2.6H2O, hexamine C6H12N4 at concentrations (0.025) M, and nickel nitrate hexahydrate (Ni (NO3)2.6H2O) solution with different concentrations was added (0%, 1%, 2%, and 4%). The all samples were implemented XRD, FESEM and UV- Vis spectrum to describe the prepared films.

3. Results and discussion

Figure 1 shows analyze changes in phase and microstructure characterize by pure ZnO and Ni doped ZnO NRs. The results are observed that well-characterized XRD peaks correspond to (100), (002), (101), (102), and (110), planes at positions 31.77, 34.47, 36, 24, 47.57 and 56.64. All diffraction obtained from the vertices ensures the formation of a hexagonal structure with space compatible with JCPDS Standard Card no1397-89 [27].

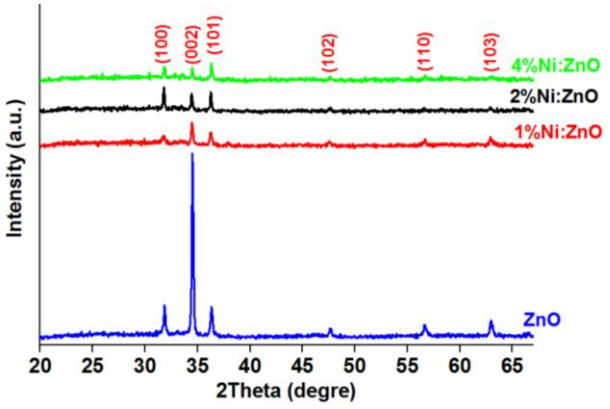

Figure 1. XRD analyze of Ni-doped ZnO nanorod, 0% Ni: ZnO (pure), 1% Ni: ZnO, 2% Ni: ZnO, 4% Ni: ZnO.

Obviously, the peak (002) indicates a favored growth direction along the c-axis, where there is no peak associated with Nickel doping appearing in the product, which indicates its successful replacement of Ni+2 ions at Zn+2locations. Moreover, Ni content has loaded the intensity of the level (002) gradually decreases, it may be representing an increase in structural disturbance due to the variance in ionic radius Ni+2 ion 0.069nm and Zn+2 ion 0.074nm [28]. The parameter micro strain(ε) calculated by equation [29]

$$\varepsilon = \frac{\beta \cos\theta}{4}, \quad (1)$$

where ε, θ and β are representing micro strain, diffraction angle and full width at half maximum, respectively. Table 1 shows parameters micro strain, about the samples Ni doped ZnO 0%, 1%, 2%, and 4% at (100), (002), and (101) direction. FESEM images were implemented to study how the inclusion content affects the morphological features of the mentioned growth films. The diameters of the samples prepared were measured by using FESEM. They were about (39.79, 56.96, 54.74and 75.65) nm for Ni-ZnO doped 0%, 1%, 2%, and 4% samples. The decreased average diameter values of nanostructured with increasing Ni content were seen, maybe due to the substitution of Zn2+ by Ni 2+ in the hexagonal lattice of ZnO [30] which further supports the XRD results.

Table 1: Structural properties of the Ni- ZnO doped based on the glass substrate.

Doping	(hkl) (101)		(002)		(100)	
	ε	2θ	ε	2θ	ε	2θ
0%	0.000874	31.85	0.00069	34.52	0.00082	36.33
1%	0.001208	31.77	0.00079	34.47	0.00099	36.24
2%	0.000805	31.78	0.00059	34.44	0.00059	36.26
4%	0.001193	33.58	0.00079	34.50	0.00079	36.32

In general, reducing the crystal size leads to an increase in the surface area, which is a useful factor for enhancing photo-catalytic activity [31]. UV-Vis spectroscopy was implemented to obtain the absorbance spectra and calculated the energy gap of the prepared samples at regions of wavelengths (350-800) nm. Figure 3 shows the absorption spectra of samples Ni-doped ZnO of (0%, 1%, 2%, and 4%) have the range edge absorption towards higher wavelengths. The results show that the mutual interaction between the band electrons and Ni2+ ions causes a redshift in the absorption edge , this agrees with [21]. The inset of figure 3 represents the absorption spectrum of the seed layer ZnO sample, where the edge absorption was about less than Ni-doped ZnO samples (0%, 1%, 2%, and 4%). The Tauc relation was used to study the optical energy gap of nickel-doped (0%, 1%, 2%, and 4%) and seed layer ZnO [32]

$$\alpha h\upsilon = A\left(h\upsilon - E_g\right)^r, \quad (2)$$

where A, r and α are represented an energy-independent constant, the nature of the transition involved and the absorption efficiency, respectively. The energy gap of Ni-doped ZnO samples0%, 1%, 2%, and 4%were about 3.2 eV,3.12eV, 3.09eV, 3 eV, respectively as shown in figure 4. It is noted that increasing Ni concentration doped ZnO is leading to a decrease in the energy gap of ZnO. The energy gap of ZnO is shifting toward the lower energy gap which can be attributed to the new ion (Ni2+) energy level

formed inside the energy gap [33]. It contraction as a function of nickel doped may be due to the

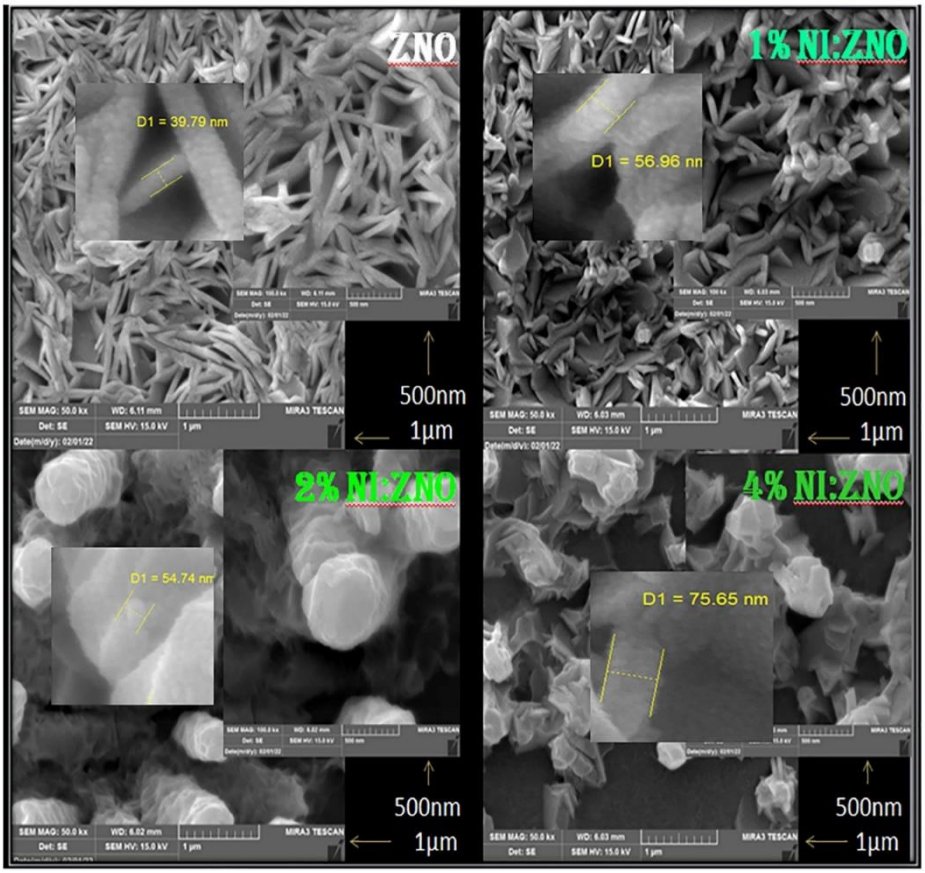

Figure 2. FESEM images for samples pure (0%) Ni: ZnO and doped (1%, 2%, 4%) Ni: ZnO.

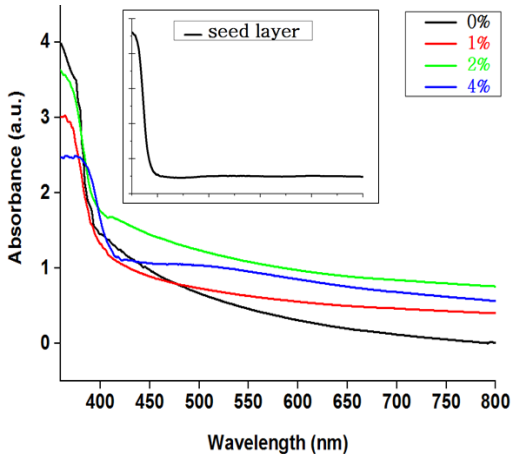

Figure 3.Optical absorption spectra for samples pure (0%) Ni: ZnO and doped (1%, 2%, 4%) Ni: ZnO and seed layer ZnO.

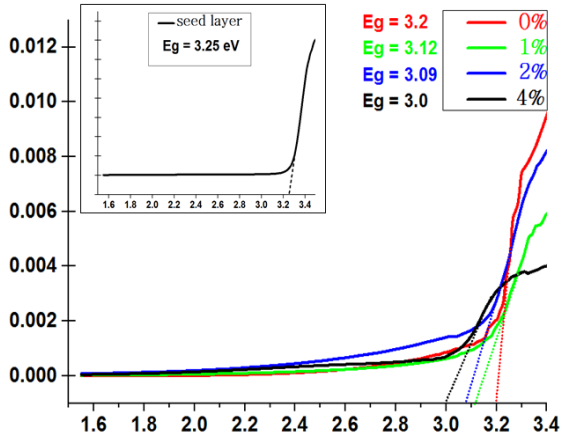

Figure 4. the energy gap for samples pure (0%) Ni: ZnO and doped (1%, 2%, 4%) Ni: ZnO and seed layer ZnO.

electronegativity difference between zinc and nickel, this electrophysiological difference generates defects in the site's defect that generate prolonged defect levels during VB and CB bounds, thus the energy gap decreases[20]. The energy gap of seed layer ZnO sample was about 3.25 eV as shown in the inset of figure 4, it may be due to the small crystal size of zinc oxide that is not grown by CBD. It should be extinction coefficient of all samples prepared was calculated by equation [34].

$$k = \frac{\lambda \alpha}{4\pi}, \quad (3)$$

where k and λ are extinction coefficient and wavelength, respectively. The nature of the extinction coefficient curves is almost similar to that of the absorption spectrum curves, because of the nature of their relationships shown in figure 5. It is noted the attenuation increases at the base absorption edge.

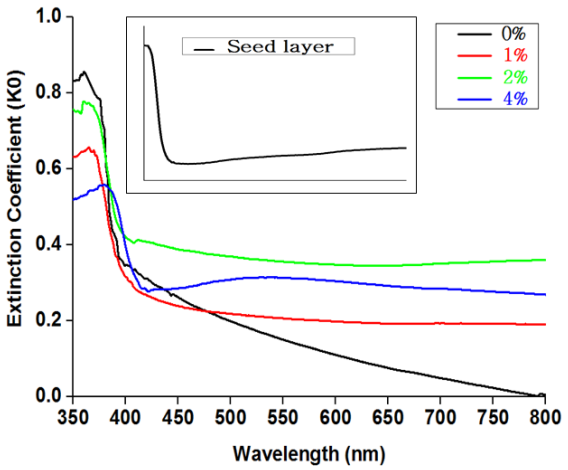

Figure 5. The extinction coefficient for samples pure (0%) Ni: ZnO and doped (1%, 2%, 4%) Ni: ZnO and seed layer ZnO.

4. Conclusions

The seed layer ZnO and Ni-doped ZnO nanostructures (0%, 1%, 2%, and 4%) were successfully grown on seeds layer ZnO/glass slides by using the CBD method at low temperature. The XRD patterns showed that the Ni+2are well combined in the synthesis of zinc oxide, no other phases of nickel were observed. FESEM photos showed zinc oxide was hexagonal structure nanorods, it showed the diameters of the Ni-doped ZnO were decreased with increasing doping ratio. The optical energy gap is shifting towards the lower energy gap (redshift) with increased the doping ratio of zinc oxide. The present research may provide an easy and cost-effective route to produce ZnO: highly efficient nickel photo catalysts. The optical results showed that the absorption at UV wavelengths and energy gap has decreased; it could be used to prepare solar cells and ultraviolet photodetectors…..etc.

References

1. A Janotti and C G Van de Walle, *Reports on progress in physics*, **72** (2009) 126501.
2. S Pearton and F Ren, *Current Opinion in Chemical Engineering*, **3** (2014) 51.
3. Q Wan, Q Li, Y Chen, T -H. Wang, X He, J Li, and C Lin, *Applied physics letters*, **84** (2004) 3654.
4. J A Anta, E Guillén, and R Tena-Zaera, *The Journal of Physical Chemistry C*, **116** (2012) 11413.
5. Y H Lin, S R Thomas, H Faber, R Li, M A McLachlan, P A Patsalas, and T D Anthopoulos, *Advanced Electronic Materials*, **2** (2016) 1600070.
6. H A Alshamarti and A H O Alkhayatt, *Materials Science in Semiconductor Processing*, **114** (2020) 105068.
7. D Nagarajan and S Venkatanarasimhan, *Environmental Science and Pollution Research*, **26** (2019) 22958.
8. S Singhal, J Kaur, T Namgyal, and R Sharma, *Physica B: Condensed Matter*, **407** (2012) 1223.
9. Y -S Kim and W -P Tai, *Applied Surface Science*, **253** (2007) 4911.
10. H A Alshamarti, L A Alasadi, and A H O Alkhayatt, in *IOP Conference Series: Materials Science and Engineering* (IOP Publishing, 2020), p. 072144.
11. A Saboor, S M Shah, and H Hussain, *Materials Science in Semiconductor Processing*, **93** (2019) 215.
12. A Buyukbas-Ulusan, İ Taşçıoğlu, A Tataroğlu, F Yakuphanoğlu, and S Altındal, *Journal of Materials Science: Materials in Electronics*, **30** (2019) 12122.
13. S Sa-Nguanprang, A Phuruangrat, T Thongtem, and S Thongtem, *Russian Journal of Inorganic Chemistry*, **64** (2019) 1841.
14. J Wang, Q Zhou, and W Zeng, *Applied Surface Science*, **479** (2019) 185.
15. M S Nadeem, T Munawar, F Mukhtar, M N ur Rahman, M Riaz, A Hussain, and F Iqbal, *Optical Materials*, **111** (2021) 110606.
16. Y Darma, S Muhammady, Y N Hendri, E Sustini, R Widita, and K Takase, *Materials Science in Semiconductor Processing*, **93** (2019) 50.
17. S E Ahn, J S Lee, H Kim, S Kim, B H Kang, K H Kim, and G T Kim, *Applied physics letters*, **84** (2004) 5022.
18. W Chen, C Yao, J Gan, K Jiang, Z Hu, J Lin, N Xu, J Sun, and J Wu, *Materials Science in Semiconductor Processing*, **109** (2020) 104918.
19. J Xie, H Wang, M Duan, and L Zhang, *Applied Surface Science*, **257** (2011) 6358.
20. W Chebil, A Gokarna, A Fouzri, N Hamdaoui, K Nomenyo, and G Lerondel, *Journal of Alloys and Compounds*, **771** (2019) 448.
21. J Rani, A Anusiya, M Praveenkumar, S Ravichandran, R K Guduru, G Ravi, and R Yuvakkumar, *Journal of Materials Science: Materials in Electronics*, **30** (2019) 731.
22. X Deng, Z Zeng, R Gao, Z Wang, G Chen, W Cai, and C Fu, *Journal of Alloys and Compounds*, **831** (2020) 154857.
23. P Bindu and S Thomas, *Journal of Theoretical and Applied Physics*, **8** (2014) 123.
24. S B Khan, S Irfan, and S -L. Lee, *Nanomaterials*, **9** (2019) 1024.
25. M Sudha, S Radha, S Kirubaveni, R Kiruthika, R Govindaraj, and N Santhosh, *Solid State Sciences* **78** (2018) 30.
26. S Fabbiyola, V Sailaja, L J Kennedy, M Bououdina, and J J Vijaya, *Journal of Alloys and Compounds*, **694** (2017) 522.
27. M Y Ali, M Khan, A T Karim, M M Rahman, and M Kamruzzaman, *Heliyon*, **6** (2020) e03588.
28. V Owoeye, E Ajenifuja, E Adeoye, G Osinkolu, and A Popoola, *Materials Research Express*, **6** (2019) 086455.
29. Z Qiao, C Agashe, and D Mergel, *Thin solid films*, **496** (2006) 520.